Journal of Theoretical Biology 601 (2025) 112044

Contents lists available at ScienceDirect

Journal of Theoretical Biology

journal homepage: www.elsevier.com/locate/yjtbi

Compartment model of strategy-dependent time delays in replicator dynamics

Małgorzata Fic [a,b,*], Frank Bastian [c], Jacek Miękisz [d], Chaitanya S. Gokhale [b,a]

[a] Department of Theoretical Biology, Max Planck Institute for Evolutionary Biology, August-Thienemann-Str. 2, Ploen, 24306, Germany
[b] Center for Computational and Theoretical Biology, University of Wuerzburg, Klara-Oppenheimer-Weg 32, Wuerzburg, 97074, Germany
[c] School of Mathematical Sciences, University College Cork, Western Road, Cork, T12 XF62, Ireland
[d] Institute of Applied Mathematics and Mechanics, University of Warsaw, ulica Banacha 2, Warsaw, 02-097, Poland

ARTICLE INFO

Dataset link: https://github.com/tecoevo/compartmentalised_timedelays

Keywords:
Evolutionary game theory
Delay differential equations
Time delays
Stationary states
Bifurcation analysis

ABSTRACT

Real-world processes often exhibit temporal separation between actions and reactions - a characteristic frequently ignored in many modelling frameworks. Adding temporal aspects, like time delays, introduces a higher complexity of problems and leads to models that are challenging to analyse and computationally expensive to solve. In this work, we propose an intermediate solution to resolve the issue in the framework of evolutionary game theory. Our compartment-based model includes time delays while remaining relatively simple and straightforward to analyse. We show that this model yields qualitatively comparable results with models incorporating explicit delays. Particularly, we focus on the case of delays between parents' interaction and an offspring joining the population, with the magnitude of the delay depending on the parents' strategy. We analyse Stag-Hunt, Snowdrift, and the Prisoner's Dilemma game and show that strategy-dependent delays are detrimental to affected strategies. Additionally, we present how including delays may change the effective games played in the population, subsequently emphasising the importance of considering the studied systems' temporal aspects to model them accurately.

1. Introduction

Evolutionary game theory provides a robust framework for modelling many biological and social interactions (Maynard Smith and Price, 1973). Traditional models largely exclude time delays, instead assuming that the actions of an individual are instantaneous and their impacts on fitness are immediate. However, real-world processes frequently exhibit temporal separation between actions and their effects across scales of biological organisation. Sporulation, the response to nutrient deprivation observed in bacteria like *Bacillus subtilis*, takes about 8 to 10 h to be completed after being triggered (Serra et al., 2014). A seed bank in weeds leads to the sprouting of plants even years after the seed has been produced (Lauenroth and Gokhale, 2023). In the animal kingdom, the delays are also abundant. In the case of marine midges *Clunio marinus*, the time between reproduction and emergence is correlated with the lunar cycle. It takes from about 15 or 30 days, as compared to their relatively short adult lives of 2 h (Kaiser et al., 2021). Similarly, pregnancy and nurturing are temporally disconnected actions that culminate in adding a new, mature individual to the population (Bateson, 1994). Social systems, too, display such delays, evident in long-term financial investments or latency in information transmission and processing (Binswanger and Carman, 2012; Bourne, 1957). Thus, incorporating temporal factors could refine evolutionary game theoretical models, capturing realistic dynamics more accurately.

The effects of time delays on replicator dynamics were discussed in Yi and Zuwang (1997), Alboszta and Miękisz (2004), Oaku (2002), Iijima (2011, 2012), Moreira et al. (2012), Miękisz and Wesolowski (2011), Miękisz et al. (2014), Wesson and Rand (2016), Wesson et al. (2016), Ben-Khalifa et al. (2018), Khalifa et al. (2016), Bodnar et al. (2020), Miękisz and Bodnar (2021) and Wettergren (2023). In Yi and Zuwang (1997), the authors introduced a social-type model in which individuals at time t imitate a strategy with a higher average payoff at time $t-\tau$ for some time delay τ. They showed that the interior stationary state of the resulting time-delayed differential equation is locally asymptotically stable for small time delays. In contrast, it becomes unstable for big ones, and oscillations appear. In Alboszta and Miękisz (2004), a biological type model was constructed in which individuals are born τ units of time after their parents played. This delay type leads to a system of equations of strategy's frequency and

* Corresponding author at: Department of Theoretical Biology, Max Planck Institute for Evolutionary Biology, August-Thienemann-Str. 2, Ploen, 24306, Germany.
E-mail address: fic@evolbio.mpg.de (M. Fic).

https://doi.org/10.1016/j.jtbi.2025.112044
Received 29 August 2024; Received in revised form 19 November 2024; Accepted 5 January 2025
Available online 10 January 2025

population size. The authors showed the absence of oscillations — the original stationary point is globally asymptotically stable for any time delay. Recently, models with strategy-dependent time delays were introduced (Moreira et al., 2012; Wesson and Rand, 2016; Khalifa et al., 2016; Bodnar et al., 2020; Miękisz and Bodnar, 2021).

In Bodnar et al. (2020) and Miękisz and Bodnar (2021), the authors discussed the biological-type model of Yi and Zuwang (1997) with strategy-dependent time delays. They reported a novel behaviour, showing that stationary states depend continuously on time delays. Moreover, at specific time delays, an interior stationary state may disappear, or another interior stationary state may appear. The equation for the stationary state of frequencies of strategies was derived and solved numerically in Miękisz and Bodnar (2021) for Stag–Hunt, Snowdrift, and Prisoner's Dilemma games. In Miękisz et al. (2023), a small-time delay approximation was proposed. The authors derived an explicit formula for the stationary state, which approximates well the exact results of Miękisz and Bodnar (2021).

Here, we introduce a model that shares the analytical tractability of Miękisz et al. (2023) without assuming small delays. We extend the approach of Miękisz and Bodnar (2021) and derive a system of ordinary differential equations that is easier to analyse through either closed-form solutions of stationary states or existing bifurcation software. In the model, time delays are represented by rates at which an offspring grows and can participate in games. More precisely, in our Kindergarten model, a newly born offspring is located in an inactive compartment. Then, with some strategy-dependent rate, juveniles become players and move to an active compartment (this is reminiscent of models of delayed protein degradation in gene expression present in Miękisz et al., 2011). This approach allows us to derive explicit analytical formulas for stationary states of the strategies. In Section 2, we recall the model of Miękisz and Bodnar (2021) and present our approach to model time delays. Results are described in Section 3, and Conclusions follow in Section 4. Notably, our model can be extended to multi-player and multi-strategy games.

2. Materials and methods

2.1. Model with explicit time delays

We begin by reintroducing the delay model constructed by Miękisz and Bodnar (2021). We will consider two-player symmetric games with two strategies: cooperation (C) and defection (D) given by the following payoff matrix:

$$\begin{array}{c} \\ C \\ D \end{array} \begin{array}{c} \begin{array}{cc} C & D \end{array} \\ \begin{pmatrix} R & S \\ T & P \end{pmatrix} \end{array}, \tag{1}$$

where the $i\,j$ entry is the payoff of the first (row) player when it plays the strategy i and the second (column) player plays the strategy j, with $i, j \in \{C, D\}$. We assume that both players are the same, and hence, payoffs of the column player are given by the matrix transposed to (1); such games are called symmetric.

Herein, we follow (Miękisz and Bodnar, 2021) closely. Let us assume that during a time interval of length ϵ, only an ϵ-fraction of the population takes part in pairwise competitions, that is, plays games. Let $p_i(t)$ with $i \in \{C, D\}$, be the number of individuals playing at time t the strategy C and D, respectively. Then $p(t) = p_C(t) + p_D(t)$ is the total number of players and $x(t) = \frac{p_C(t)}{p(t)}$ is the fraction of the population playing C. The expected payoffs of an individual is given by,

$$U_C(t) = Rx(t) + S\,(1 - x(t))\,, \tag{2}$$

and

$$U_D(t) = Tx(t) + P\,(1 - x(t))\,, \tag{3}$$

for cooperators and defectors, respectively.

We consider that individuals are born sometime after their parents interact. Further, we assume that time delays depend on strategies and are equal to τ_C and τ_D respectively. Miękisz and Bodnar (2021) proposed that the growth of the population playing a particular strategy is given as

$$p_i(t + \epsilon) = (1 - \epsilon)p_i(t) + \epsilon p_i(t - \tau_i)U_i(t - \tau_i); i = C, D. \tag{4}$$

and derive a system of coupled delayed differential equations for the fraction using the first strategy $x(t)$ and the population size $p(t)$,

$$\begin{aligned} \frac{dx(t)}{dt} &= \frac{x(t - \tau_C)p(t - \tau_C)U_C(t - \tau_C)\,(1 - x(t))}{p(t)} \\ &\quad - \frac{\left(1 - x(t - \tau_D)\right)\,p(t - \tau_D)U_D(t - \tau_D)x(t)}{p(t)}, \end{aligned} \tag{5}$$

$$\frac{dp(t)}{dt} = -p(t) + p_C(t - \tau_C)U_C(t - \tau_C) + p_D(t - \tau_D)U_D(t - \tau_D). \tag{6}$$

Then, the authors provided an equation for the stationary state of x and solved it numerically for various games.

Here, we propose another type of model to deal with time delays. We do not have to track the population size, and we can derive analytical formulas for the frequency of strategies in stationary states. This provides more insight into the dynamics of more complex games and can easily be expanded to multi-player and multi-strategy games.

2.2. Kindergarten compartment model

In the Kindergarten model, a large but finite population is considered. Individuals in the population take part in pairwise interactions, play games, and obtain payoff. The payoff is, in turn, translated into several identical offspring created. The newly created offspring are placed in an inactive compartments (kindergartens) and rejoin the active compartment (adult population) upon maturation, with per capita rate $1/\tau_i$ for $i \in \{C, D\}$, as shown in Fig. 1. Importantly, the adult population is well-mixed so that cooperators and defectors can interact with one another.

Let us denote by k_i sizes of kindergartens for offspring which inherited the ith strategy with $i \in \{C, D\}$. Then, let $y_i = k_i/p$ for $i \in \{C, D\}$ denote kindergartens' sizes relative to the adult population. Notably, the sum of $y_i(\hat{t})$ for all i does not have to be equal to 1, since the variables are not fractions of the population. The list of variables used in the model and corresponding units are presented in Table 1.

We assume that in a small time interval ϵ only a fraction $\delta_K(\epsilon)$ of juveniles in the kindergarten can mature, with δ_K being a function such that $\frac{d\delta_K(\epsilon)}{d\epsilon} \geq 0$, $\delta_K(0) = 0$, $\frac{d\delta_K(0)}{d\epsilon} = const$. That is, in a given time interval, at least as many individuals have to mature as in the shorter interval; no juveniles can mature instantly. Similarly, in a time interval ϵ only a $\delta_P(\epsilon)$ fraction of the adult population takes part in the game with δ_P being a function such that $\frac{d\delta_P(\epsilon)}{d\epsilon} \geq 0$, $\delta_P(0) = 0$ and $\frac{d\delta_K(0)}{d\epsilon} = const$. That is, any interactions that have taken place in a shorter time interval have also occurred in a longer time, and there are no instantaneous interactions. Hence, in the Kindergarten model, we relax the assumption made by Miękisz and Bodnar (2021) on the fraction of individuals partaking in the game.

Then, the size of the kindergarten of strategy i at time $t + \epsilon$ is equal to:

$$k_i(\hat{t} + \epsilon) = \left(1 - \frac{\delta_K(\epsilon)}{\tau_i}\right) k_i(\hat{t}) + \delta_P(\epsilon)p_i(\hat{t})U_i(\hat{t}). \tag{7}$$

Similarly, the change in the size of the adult population using strategy i can be calculated as:

$$p_i(\hat{t} + \epsilon) = (1 - \delta_P(\epsilon))p_i(\hat{t}) + \frac{\delta_K(\epsilon)}{\tau_i} k_i(\hat{t}). \tag{8}$$

The size of the whole adult population follows:

$$p(\hat{t} + \epsilon) = (1 - \delta_P(\epsilon))p(\hat{t}) + \frac{\delta_K(\epsilon)}{\tau_C} k_C(\hat{t}) + \frac{\delta_K(\epsilon)}{\tau_D} k_D(\hat{t}). \tag{9}$$

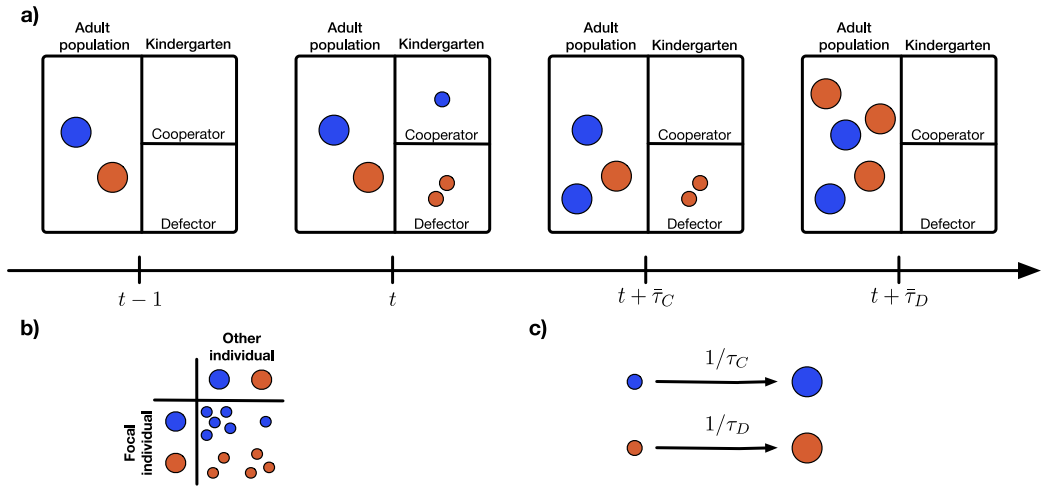

Fig. 1. (a) Individuals in the adult population interact with one another and receive payoff (offspring) based on those interactions. Offspring created at time t join the strategy-specific compartment called a kindergarten. After an offspring matures, it joins the adult population and can reproduce. The average maturation time is denoted by $\bar{\tau}_i$ for $i \in \{C, D\}$ (b) The payoff matrix indicates the expected number of offspring created in each interaction. (c) Maturation rate depends on the parent's strategy and equals $1/\tau_C$ and $1/\tau_D$ for cooperators and defectors, respectively.

Now we can derive equation for change in $x(\hat{t})$, $y_C(\hat{t})$ and $y_D(\hat{t})$.

$$x(\hat{t}+\epsilon) - x(\hat{t}) = \frac{(1-\delta_P(\epsilon))p_C(\hat{t}) + \frac{\delta_K(\epsilon)}{\tau_C}k_C(\hat{t})}{(1-\delta_P(\epsilon))p(\hat{t}) + \frac{\delta_K(\epsilon)}{\tau_C}k_C(\hat{t}) + \frac{\delta_K(\epsilon)}{\tau_D}k_D(\hat{t})} - \frac{p_C(\hat{t})}{p(\hat{t})} \tag{10}$$

$$y_i(\hat{t}+\epsilon) - y_i(\hat{t}) = \frac{(1-\frac{\delta_K(\epsilon)}{\tau_i})k_i(\hat{t}) + \delta_P(\epsilon)p_i(\hat{t})U_i(\hat{t})}{(1-\delta_P(\epsilon))p(\hat{t}) + \frac{\delta_K(\epsilon)}{\tau_C}k_C(\hat{t}) + \frac{\delta_K(\epsilon)}{\tau_D}k_D(\hat{t})} - \frac{k_i(\hat{t})}{p(\hat{t})} \tag{11}$$

After some rearrangements, we divide both sides of the equations by ϵ and take the limit of $\epsilon \to 0$ and obtain the following differential equations:

$$\frac{dx(\hat{t})}{d\hat{t}} = \frac{d\delta_K(0)}{d\epsilon}\frac{\frac{1}{\tau_C}k_C(\hat{t})(p(\hat{t}) - p_C(\hat{t})) - p_C(\hat{t})\frac{1}{\tau_D}k_D(\hat{t})}{p^2(\hat{t})} \tag{12}$$

$$\frac{dy_i(\hat{t})}{d\hat{t}} = \frac{d\delta_P(0)}{d\epsilon}\frac{p(\hat{t})(k_i(\hat{t}) + p_i(\hat{t})U_i(\hat{t}))}{p^2(\hat{t})} - \frac{d\delta_K(0)}{d\epsilon}\frac{k_i(\hat{t})(\frac{p(\hat{t})}{\tau_i} + \frac{k_C(\hat{t})}{\tau_C} + \frac{k_D(\hat{t})}{\tau_D})}{p^2(\hat{t})} \tag{13}$$

Now we denote $\frac{d\delta_P(0)}{d\epsilon} = Q$ and $\frac{d\delta_K(0)}{d\epsilon} = K$ and recall that $Q \geq 0$ and $K \geq 0$. Then, after rearrangements, we get

$$\begin{aligned}
\frac{dx(\hat{t})}{d\hat{t}} &= K\left(\frac{y_C(\hat{t})(1-x(\hat{t}))}{\tau_C} - \frac{x(\hat{t})y_D(\hat{t})}{\tau_D}\right)\\
\frac{dy_C(\hat{t})}{d\hat{t}} &= Q\left(y_C(\hat{t}) + x(\hat{t})U_C(\hat{t})\right)\\
&\quad - Ky_C(\hat{t})\left(\frac{1}{\tau_C} + \frac{y_C(\hat{t})}{\tau_C} + \frac{y_D(\hat{t})}{\tau_D}\right)\\
\frac{dy_D(\hat{t})}{d\hat{t}} &= Q\left(y_D(\hat{t}) + (1-x(\hat{t}))U_D(\hat{t})\right)\\
&\quad - Ky_D(\hat{t})\left(\frac{1}{\tau_D} + \frac{y_C(\hat{t})}{\tau_C} + \frac{y_D(\hat{t})}{\tau_D}\right)
\end{aligned} \tag{14}$$

For simplicity, in this work, we assume that $Q = K$.

Next, we rescale time by introducing

$$t = a\hat{t}, \to \hat{t} = \frac{t}{a}.$$

By the chain rule, we have

$$\frac{dx}{dt} = \frac{dx}{d\hat{t}}\frac{d\hat{t}}{dt} = \frac{1}{a}\frac{dx}{d\hat{t}},$$
$$\frac{dy_i}{dt} = \frac{dy_i}{d\hat{t}}\frac{d\hat{t}}{dt} = \frac{1}{a}\frac{dy_i}{d\hat{t}}.$$

Setting $a = Q$, we obtain our final Kindergarten model:

$$\begin{aligned}
\frac{dx(t)}{dt} &= \frac{y_C(t)\,(1-x(t))}{\tau_C} - \frac{y_D(t)x(t)}{\tau_D},\\
\frac{dy_C(t)}{dt} &= y_C(t)\left(\frac{\tau_C - 1}{\tau_C} - \frac{y_C(t)}{\tau_C} - \frac{y_D(t)}{\tau_D}\right) + x(t)U_C(t),\\
\frac{dy_D(t)}{dt} &= y_D(t)\left(\frac{\tau_D - 1}{\tau_D} - \frac{y_C(t)}{\tau_C} - \frac{y_D(t)}{\tau_D}\right) + (1-x(t))\,U_D(t).
\end{aligned} \tag{15}$$

Similarly, we can obtain the differential equation for the change in population size, given by:

$$\frac{dp(t)}{dt} = p(t)\left(\frac{y_C(t)}{\tau_C} + \frac{y_D(t)}{\tau_D} - 1\right). \tag{16}$$

Hence, the size of the population in a stationary state of frequencies x^*, y_C^*, y_D^*, $p(t) = p(0)e^{(y_C^*/\tau_C + y_D^*/\tau_D - 1)t}$ grows exponentially if

$$\frac{y_C^*(t)}{\tau_C} + \frac{y_D^*(t)}{\tau_D} > 1, \tag{17}$$

or goes extinct otherwise. Hence, condition (17) has to be met for the population not to go extinct.

We should take care of cases where one delay equals zero. For $\tau_C = 0$ there is no cooperator kindergarten ($y_C = 0$) and the system (15) becomes:

$$\begin{aligned}
\frac{dx(t)}{dt} &= x(t)\left(U_C(t)(1-x(t)) - \frac{y_D(t)}{\tau_D}\right),\\
\frac{dy_C(t)}{dt} &= 0,\\
\frac{dy_D(t)}{dt} &= y_D(t)\left(\frac{\tau_D - 1}{\tau_D} - x(t)U_C(t) - \frac{y_D(t)}{\tau_D}\right) + (1-x(t))\,U_D(t).
\end{aligned} \tag{18}$$

Analogously, for $\tau_D = 0$ the defector kindergarten is empty ($y_D = 0$) and the system (15) becomes:

$$\begin{aligned}
\frac{dx(t)}{dt} &= \frac{y_C(t)}{\tau_C} - x(t)\left((1-x(t))U_D(t) + \frac{y_C(t)}{\tau_C}\right),\\
\frac{dy_C(t)}{dt} &= y_C(t)\left(\frac{\tau_C - 1}{\tau_C} - (1-x(t))U_D(t) - \frac{y_C(t)}{\tau_C}\right) + x(t)U_C(t),\\
\frac{dy_D(t)}{dt} &= 0.
\end{aligned} \tag{19}$$

The system of Eqs. (15) has two trivial stationary states, $x = 1, 0$, of full cooperation and defection, and two possible internal stationary states whose existence depends on the game parameters and delays.

For strategy-independent delays, i.e. $\tau_C = \tau_D$, our equations simplify greatly, and the system has only one possible internal stationary

Table 1
Variables used in the Kindergarten model and corresponding units.

Variable	Unit	Description
p_i	player	Number of players playing strategy i for $i \in \{C, D\}$
x	dim less	Ratio of players playing cooperate in p
k_i	player	Number of players in the kindergarten of strategy i for $i \in \{C, D\}$
y_i	dim less	Relative size of the kindergarten k_i with respect to the total population p for $i \in \{C, D\}$
$1/\tau_i$	dim less	Maturation rate of individuals playing strategy i for $i \in \{C, D\}$
$\bar{\tau}_i$	time	Average maturation time of individuals playing strategy i for $i \in \{C, D\}$
ϵ	time	Small time interval
δ_P	dim less	Proportion of the adult population participating in the game in the given time interval
δ_K	dim less	Fraction of kindergarten maturing in the given time interval
Q	1/time	$\frac{d\delta_P(0)}{dt}$
K	1/time	$\frac{d\delta_K(0)}{dt}$
U_i	dim less	Expected payoff of an individual playing strategy i for $i \in \{C, D\}$
R, S, T, P	dim less	Payoffs defined by the payoff matrix (1)

state: $x^* = (P-S)/(R-T+P-S)$ equal to the one for replicator dynamics without time delays. Hence, in this work, we only focus on strategy-dependent delays, i.e. $\tau_C \neq \tau_D$.

In the following, we study Eqs. (15) through the lenses of dynamical systems and bifurcation theory. That is, we investigate stationary states of Eqs. (15) and perform a linear stability analysis of their stability (Glendinning, 1994). They might be given in a closed form for special payoff matrices, allowing us to analyse the dependence of the stationary states on delays and payoff matrix entries. In the case of a general payoff matrix, stationary states are calculated numerically (Julia package BifurcationKit Veltz, 2020). In particular, we consider three specific games, Stag–Hunt, Snowdrift, and the Prisoner's Dilemma one.

3. Results

3.1. Stag–Hunt game

In the Stag–Hunt game, two individuals decide between cooperating and hunting a stag together (C) or pursuing a hare independently (D). Hunting a hare does not require help from the other individual and results in a specific payoff b; however, a stag provides a higher payoff value a (Skyrms, 2004). The following payoff matrix characterises the Stag–Hunt game:

$$\begin{array}{cc} & \begin{array}{cc} C & D \end{array} \\ \begin{array}{c} C \\ D \end{array} & \begin{pmatrix} R=a & S=0 \\ T=b & P=b \end{pmatrix} \end{array} \tag{20}$$

where $a > b > 0$. In the case of no delays, i.e. $\tau_D = \tau_C = 0$, Eq. (15) collapses to a well-studied replicator dynamics with two asymptotically stable stationary states, $x_0 = 0$ and $x_1 = 1$, and an unstable one, $x_2 = b/a$. For the Stag–Hunt game with delays, the system (15) becomes:

$$\begin{aligned} \frac{dx(t)}{dt} &= \frac{y_C(t)(1-x(t))}{\tau_C} - \frac{y_D(t)x(t)}{\tau_D}, \\ \frac{dy_C(t)}{dt} &= y_C\left(\frac{\tau_C - 1}{\tau_C} - \frac{y_C(t)}{\tau_C} - \frac{y_D(t)}{\tau_D}\right) + ax^2(t), \\ \frac{dy_D(t)}{dt} &= y_D\left(\frac{\tau_D - 1}{\tau_D} - \frac{y_C(t)}{\tau_C} - \frac{y_D(t)}{\tau_D}\right) + b(1-x(t)). \end{aligned} \tag{21}$$

The system (21) may have three stationary states in $[0,1]^3$. The full defection stationary state $x_0 = 0$ becomes

$$e_0 = \left(0, 0, \frac{1}{2}\left(\tau_D - 1 + \sqrt{4b\tau_D + \tau_D^2 - 2\tau_D + 1}\right)\right). \tag{22}$$

For the condition (17) to be met and the population in this stationary state to grow exponentially, the following needs to be true:

$$\frac{1}{2\tau_D}\left(\tau_D - 1 + \sqrt{4b\tau_D + \tau_D^2 - 2\tau_D + 1}\right) > 1. \tag{23}$$

Thus, an additional condition needs to hold: $b \geq 1$. The full cooperation stationary state x_1 becomes

$$e_1 = \left(1, \frac{1}{2}\left(+\tau_C - 1 + \sqrt{4a\tau_C + \tau_C^2 - 2\tau_C + 1}\right), 0\right). \tag{24}$$

Again, we check the condition (17), which in this stationary state becomes:

$$\frac{1}{2\tau_C}\left(\tau_C - 1 + \sqrt{4a\tau_C + \tau_C^2 - 2\tau_C + 1}\right) > 1. \tag{25}$$

For the condition to held, we need an additional constraint: $a \geq 1$. Lastly, the internal stationary state x_2 takes the following form:

$$e_2 = \left(x_2^*, \frac{\tau_C x_2^* y_D^*}{\tau_D(1-x_2^*)}, y_D^*\right) \tag{26}$$

where

$$\begin{aligned} x_2^* &= \frac{\tau_C + (\tau_D - \tau_C)\sqrt{(4b-2)\tau_D + \tau_D^2 + 1}}{2a\tau_D^2} \\ &\quad + \frac{2b\tau_C - \tau_C + \tau_D - 1}{2a\tau_D}, \end{aligned} \tag{27}$$

$$y_D^* = \frac{(1-x_2^*)\tau_D\left(\tau_C - 1 + \sqrt{(4ax-2)\tau_C + \tau_C^2 + 1}\right)}{2\tau_C}. \tag{28}$$

For the condition (17) to be met in e_2, that is for

$$\frac{\tau_C x_2^* y_D^*}{\tau_D \tau_C (1-x_2^*)} + \frac{y_D^*}{\tau_D} > 1 \tag{29}$$

to hold true, we need $x_2^* \geq 1/a$. For the population to grow exponentially, we have to have $a, b > 1$ and $x_2^* \geq 1/a$.

Homogeneous stationary states. We conduct stability analysis of e_0 and show that it is always a stable stationary state. The stationary state e_1 is stable unless the following condition is met: $\tau_C \geq m$ where

$$m = \frac{(a-b)\sqrt{4b\tau_D + \tau_D^2 - 2\tau_D + 1} + a(2b-1)\tau_D + a - b\left(\tau_D + 1\right)}{2(b-1)b}. \tag{30}$$

For a large enough cooperator delay, full cooperation loses its stability, and the internal stationary states vanish. Details of the analysis are presented below and in Appendix A.1.

Internal stationary state. If no delays are present, the internal stationary point x_2^* always exists and equals b/a. The increase of τ_C leads to an increase in the stationary point value. Then, the stationary state reaches full cooperation ($x_2^* = 1$) and disappears when $\tau_C = m$. An increase in τ_D always leads to a decrease in x_2^*. In the limiting case of $\tau_D \to \infty$ we have $x_2^* \to 1/a$. The latter result ensures that condition (17) is met for the internal stationary state. When the internal stationary state e_2 exists, it is always unstable, as shown in Appendix A.1.

One delay present. We consider the limiting case of each delay to be equal to 0. We solve the systems (18) for $\tau_C = 0$ and (19) for $\tau_D = 0$ and

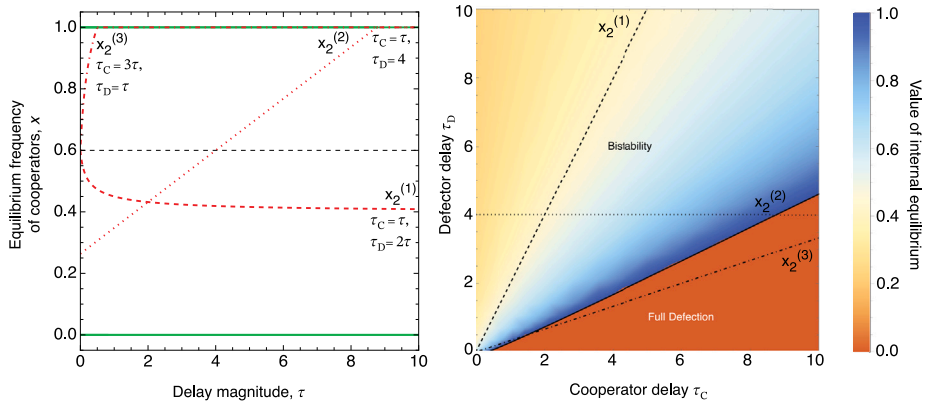

Fig. 2. Stability of the stationary states of the Stag–Hunt game represented by matrix (35). On the left, the stationary state values for the specific values of delays are plotted. The dashed line represents the internal stationary state $x_2^{(1)}$ as a function of τ, when $\tau_C = \tau$, $\tau_D = 2\tau$. An increase in τ leads to a decrease in stationary state value. The dotted line represents internal stationary state $x_2^{(2)}$ as a function of τ, when $\tau_C = \tau$, $\tau_D = 4$. The internal stationary state disappears for big enough τ, and full cooperation loses its stability. The dot-dashed line represents the internal stationary state $x_2^{(3)}$ as a function of τ, when $\tau_D = \tau$, $\tau_C = 3\tau$. An increase in τ leads to an increase in the stationary state value until its disappearance. On the right, the stability of the system in the parameter space τ_C and τ_D is shown. The solid black line indicates the point of bifurcation. In the "Full Defection" region, only e_0 is stable. In the "Bistability" region, both e_0 and e_1 are stable, and their basins of attraction are divided by the unstable internal stationary state. The colour indicates the value of the internal stationary state. The values considered on the left are represented by dashed ($x_2^{(1)}$), dotted ($x_2^{(2)}$) and dot-dashed ($x_2^{(3)}$) lines, respectively. The effects of only one delay can be observed on the left and bottom edges of the plot.

check the behaviour of e_2 in the corresponding limits. If it exists, the internal stationary state of the system (18) takes the following form:

$$\tilde{e}_2 = \left(\tilde{x}_2, 0, a\tau_D(1-\tilde{x}_2)\tilde{x}_2\right) \tag{31}$$

where

$$\tilde{x}_2 = \frac{\tau_D - 1 + \sqrt{4b\tau_D + \tau_D^2 - 2\tau_D + 1}}{2a\tau_D}. \tag{32}$$

The solution coincides with the value of e_2 in the limit of $\tau_C \to 0$. Additionally, we can show that: $\lim_{\tau_D \to 0} \tilde{x}_2 = b/a$. Hence, in the limiting case of no delays, we recover the solution of the standard Stag–Hunt game. Similarly, for $\tau_D = 0$, we solve the system (19). The system has only one stationary solution in the game-theoretic relevant interval of $\bar{x} \in (0, 1)$:

$$\bar{e}_2 = (\bar{x}_2, b\tau_C\bar{x}_2, 0) \tag{33}$$

where

$$\bar{x}_2 = \frac{b(b\tau_C - \tau_C + 1)}{a}. \tag{34}$$

Again, we can show that $\lim_{\tau_D \to 0} x_2^* = \bar{x}_2$ and $\lim_{\tau_C \to 0} \bar{x}_2 = b/a$. So, the internal solution represented by e_2 can be used in the limiting cases of either or both delays approaching 0.

We show that in the classical Stag–Hunt game, the introduction of delay is insufficient to destabilise complete defection. However, it is possible to destabilise full cooperation. Moreover, we prove that increasing the delay of one of the strategies shrinks the basin of attraction of the stationary state consisting of individuals following only that strategy.

Example. Below, we present an analysis of the Stag–Hunt game characterised by the following payoff matrix:

$$\begin{array}{cc} & \begin{array}{cc} C & D \end{array} \\ \begin{array}{c} C \\ D \end{array} & \begin{pmatrix} R = 5 & S = 0 \\ T = 3 & P = 3 \end{pmatrix} \end{array} \tag{35}$$

In the case of no delay, the game has two stable stationary states corresponding to the two homogeneous states. The unstable stationary state, dividing the basins of attraction of the two stationary states, is $x^* = 0.6$.

Fig. 2 explores the change in the stability of the stationary states of the system (21) in the parameter space of the delays. In most of the parameter space, we observe full cooperation and defection bistability. The value of x_2^* decreases with τ_D, reaching the limiting value of 0.2 $(1/a)$. With the increase in τ_C, the value of the x_2^* increases. As the internal stationary state value approaches 1, one of the stable stationary states disappears, leaving full defection as the only stable stationary state. The curve dividing the region of bistability and full defection marks the bifurcation point.

3.2. Snowdrift game

Next, we analyse the Snowdrift game, also known as the chicken game or the hawk-dove game. In this game, two players choose between contributing to a common good (C) or not (D). The cost of the good (c) is divided equally between all contributors. If at least one of the individuals contributes, each player, regardless of their strategy, obtains the benefit b (Osborne et al., 2004). Hence, the game can be represented by the following matrix:

$$\begin{array}{cc} & \begin{array}{cc} C & D \end{array} \\ \begin{array}{c} C \\ D \end{array} & \begin{pmatrix} R = b - c/2 & S = b - c \\ T = b & P = 0 \end{pmatrix} \end{array} \tag{36}$$

where $b > c > 0$. The game with no delays has two unstable stationary states $x_0 = 0$, $x_1 = 1$ and one stable internal stationary state $x_2 = (b-c)/(b-c/2)$.

For the payoffs specified in the matrix (36) the system (15) becomes:

$$\begin{aligned} \frac{dx(t)}{dt} &= \frac{y_C(t)(1-x(t))}{\tau_C} - \frac{y_D(t)x(t)}{\tau_D} \\ \frac{dy_C(t)}{dt} &= y_C\left(\frac{\tau_C - 1}{\tau_C} - \frac{y_C(t)}{\tau_C} - \frac{y_D(t)}{\tau_D}\right) + x(t)\left(\frac{c}{2}x(t) + b - c\right) \\ \frac{dy_D(t)}{dt} &= y_D\left(\frac{\tau_D - 1}{\tau_D} - \frac{y_C(t)}{\tau_C} - \frac{y_D(t)}{\tau_D}\right) + bx(t)(1-x(t)). \end{aligned} \tag{37}$$

This system (37) can have four stationary states. The trivial stationary state x_0 becomes:

$$e_0 = \left(0, 0, \tau_D - 1\right), \tag{38}$$

if $\tau_D > 1$. The population would grow exponentially if $1/\tau_D < 0$. Additionally, when $\tau_D \leq 1$, $y_D = 0$. As the delay cannot take negative values, we can see that the population always goes extinct in the full defection stationary state.

The full cooperation stationary state x_1 becomes:

$$e_1 = \left(1, \frac{1}{2}\left(\tau_C - 1 + \sqrt{\tau_C(4b - 2c + \tau_C - 2) + 1}\right), 0\right). \tag{39}$$

In the full cooperation stationary state, the condition (17) becomes:

$$\frac{1}{2\tau_C}\left(\tau_C - 1 + \sqrt{\tau_C(4b - 2c + \tau_C - 2) + 1}\right) > 1 \tag{40}$$

and holds when $(1 < b < 2 \wedge 0 < c \leq 2b - 2) \vee (b \geq 2)$. Additionally, two internal stationary states may be present:

$$e_2 = \left(x_2^*, \frac{\tau_C x_2^* y_D^{(2)}}{\tau_D - \tau_D x_2^*}, y_D^{(2)}\right) \tag{41}$$

$$e_3 = \left(x_3^*, \frac{\tau_C x_3^* y_D^{(1)}}{\tau_D - \tau_D x_3^*}, y_D^{(3)}\right) \tag{42}$$

where

$$\begin{aligned} x_2^* = {} & \frac{1}{(c\tau_D - 2b\tau_C)^2} \\ & \Big((\tau_C - \tau_D)\sqrt{o} \\ & + \tau_D\left(4b^2\tau_C - 2b(2c\tau_C + \tau_C - 1) - c(\tau_C + 1)\right) \\ & + \tau_C(2b(\tau_C - 1) + c) + c\tau_D^2(-2b + 2c + 1)\Big), \end{aligned} \tag{43}$$

$$\begin{aligned} x_3^* = {} & \frac{1}{(c\tau_D - 2b\tau_C)^2} \\ & \Big((\tau_D - \tau_C)\sqrt{o} \\ & + \tau_D\left(4b^2\tau_C - 2b(2c\tau_C + \tau_C - 1) - c(\tau_C + 1)\right) \\ & + \tau_C(2b(\tau_C - 1) + c) + c\tau_D^2(-2b + 2c + 1)\Big), \end{aligned} \tag{44}$$

$$y_d^{(i)} = \frac{1}{2}(1 - x_i^*)\left(\tau_D - 1 + \sqrt{4b\tau_D x + \tau_D^2 - 2\tau_D + 1}\right). \tag{45}$$

In (43) and (44) o is defined as:

$$\begin{aligned} o = {} & 16b^3\tau_C + 4b^2(\tau_C(-4c + \tau_C - 2) - 2c\tau_D + 1) \\ & + 4bc(2c\tau_D + \tau_C(-\tau_D) + \tau_C + \tau_D - 1) + c^2(\tau_D - 1)^2. \end{aligned} \tag{46}$$

In the internal equilibria, the condition (17) takes the following form:

$$\frac{x_i^* y_D^{(i)}}{\tau_D - \tau_D x_i^*} + \frac{y_D^{(i)}}{\tau_D} > 1. \tag{47}$$

The condition is met when one of the following constraints holds true:

$$\begin{aligned} & \Big(1 < b \leq 2 \wedge \Big((0 < c \leq b - 1) \\ & \vee \left(b - 1 < c < 2b - 2 \wedge \frac{-2b + 2c + 2}{c} \leq x_i^* < 1\right)\Big)\Big), \\ & \Big(b > 2 \wedge \Big((0 < c \leq b - 1) \\ & \vee \left(b - 1 < c < b \wedge \frac{-2b + 2c + 2}{c} \leq x_i^* < 1\right)\Big)\Big). \end{aligned} \tag{48}$$

Now, we combine conditions (40) and (48) and obtain the following constrains on the game parameters: $(1 < b \leq 2 \wedge c < 2b - 2) \vee b > 2$. Additionally, when $b < c + 1$, the following constraint needs to be applied to the internal stationary state values: $\frac{-2b+2c+2}{c} \leq x_i^*$ for $i \in \{2, 3\}$.

Homogeneous stationary states. The analysis of the full cooperation stationary state e_1 shows that it is stable if $\tau_D > n$ where $n = \frac{4b^2\tau_C - 2bc\tau_C - 4b\tau_C + c\tau_C + c}{4b^2 - 4bc - 4b + c^2 + 2c} + \sqrt{\frac{4bc^2\tau_C - 2c^3\tau_C + c^2\tau_C^2 - 2c^2\tau_C + c^2}{(4b^2 - 4bc - 4b + c^2 + 2c)^2}}$. Hence, full cooperation can be stable if the defector delay is large enough and the cooperator delay is small enough. We show that full defection stationary state e_0 is stable if the following conditions are met $(0 < c \leq 2 \wedge (2 + c)/c < b < c + 1 \wedge \tau_D > p) \vee (c > 2 \wedge c < b < c + 1 \wedge \tau_D > p)$ where $p = \frac{1}{2}\sqrt{\frac{4b\tau_C - 4c\tau_C + \tau_C^2 - 2\tau_C + 1}{(b-c-1)^2}} + \frac{-\tau_C - 1}{2(b-c-1)}$ and is never stable if $\tau_D < 1$. The specific form of the payoff matrix of the Snowdrift game violates the assumption of exponential growth whenever full defection is in a stable stationary state. Therefore, any parameter combination leading to stability of full defection needs to be noted as leading to the possible extinction of the population. As population extinction is excluded from the model's assumptions, we only analyse the parameter space when extinction is impossible. Hence, we assume that $b \geq c + 1$. The details of the stability analysis are presented in Appendix A.2.

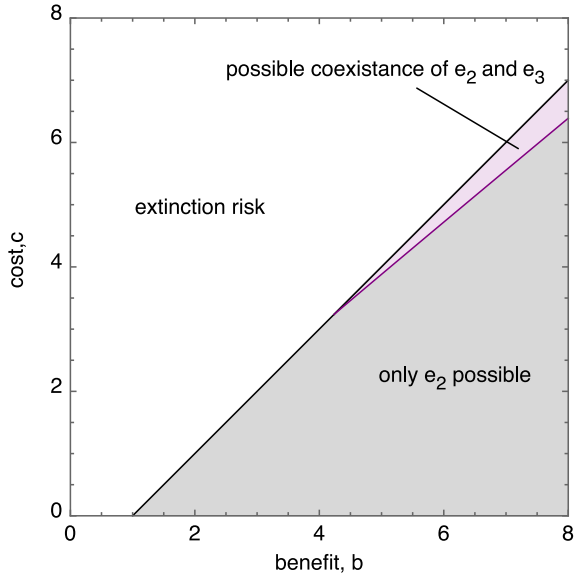

Fig. 3. The existence of one or two internal in the Snowdrift game parameter (b and c) space. In the grey region, only e_2 can exist. In the purple region, both e_2 and e_3 may exist. Outside of the coloured region, the population is at risk of extinction.

Internal stationary state. We analyse the two possible internal (in the interval $(0, 1)$) stationary states (e_2, e_3). When the cooperator delay exceeds the defector delay ($\tau_C > \tau_D$), only one internal stationary state, e_2, exists. In that region of the parameter space, the stationary state is always stable. With the increase of cooperator delay, the internal stationary state value x_2^* decreases. In the limit of $\tau_C \to \infty$ x_2^* approaches a limiting value $1/b$. Notably, for all considered game parameters $1/b > (-2b + 2c + 2)/c$, the population grows exponentially in the internal stationary state. An increase in the defector delay τ_D leads to an increase in the value of x_2^*. In the limit of the delay τ_D approaching τ_C, the stationary state approaches the limiting value, the internal stationary state of the system with no delays, $(b - c)/(b - c/2)$.

If the defector delay is greater than the cooperator delay ($\tau_D > \tau_C$), both internal stationary states may exist in the interesting interval $(0, 1)$. In particular, the existence of the stationary state e_3 depends on the parameter values of the game: the stationary state can exist only if certain conditions are met. Otherwise, only e_2 can exist. The two regions of the b, c parameter space are represented in Fig. 3. Both internal stationary states may exist in the parameter region indicated in purple in Fig. 3. Particularly, when $0 < \tau_C < q$, where $q = \frac{8b^3 - 4b^2(3c+2) + 4bc(c+2) - c^2}{2\sqrt{2}\sqrt{b(2b^3 - 2b^2(2c+1) + bc(2c+3) - c^2)}} - 2b + c + 1$ the two stationary states coexist, with $x_2^* < x_3^*$, e_2 being stable and e_3 unstable. At the point $o = 0$, where o has been defined as (46), the two stationary states collide at a fold bifurcation and disappear. e_3 collides with the full cooperation stationary state e_1 at $\tau_D = n$ and the two switch stability. In the gray region in Fig. 3 or when $\tau_C \geq q$ only e_2 exists. The value of x_2^* decreases with cooperator delay τ_C and increases with defector delay τ_D, colliding with the full cooperation stationary state at $\tau_D = n$. In the limit of $\tau_C \to \tau_D$ the fraction of the cooperators approaches $(b - c)/(b - c/2)$. If it exists, the internal stationary state is always stable.

One delay present. To analyse the system (18), we must consider the game parameter values and the two regions in Fig. 3. In the grey region, only one internal stationary state can exist, the fraction of cooperators coinciding with x_2^* in the limit of $\tau_C \to 0$:

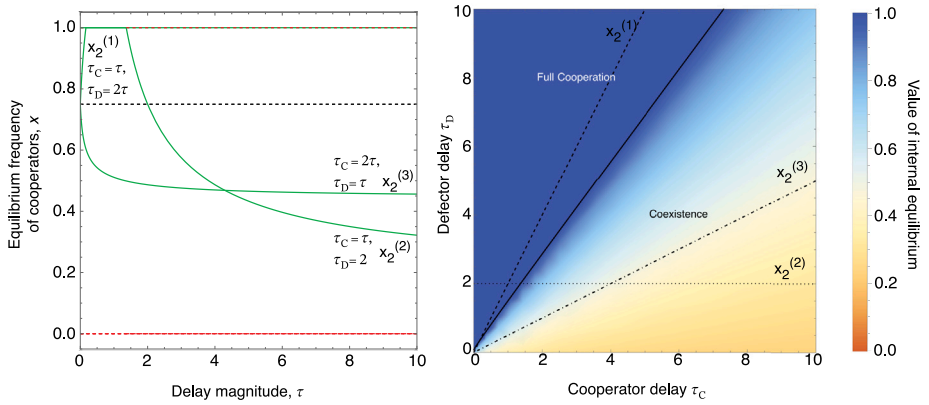

Fig. 4. Stability of the stationary states of the Snowdrift game represented by matrix (52). On the left, the stationary state values for specific delays are plotted. The $x_2^{(1)}$ line represents the internal stationary state as a function of τ, when $\tau_C = \tau$, $\tau_D = 2\tau$. An increase in τ leads to an increase in stationary state value. The internal stationary state ceases to exist for a high enough value of τ, and full cooperation becomes stable. The $x_2^{(2)}$ line represents internal stationary state as a function of τ, when $\tau_C = \tau, \tau_D = 2$. Full cooperation is a stable stationary state for small values of τ, and no internal stationary state exists. A stable internal stationary state appears with the increase in τ, and full cooperation loses stability. The value of the internal stationary state decreases with the increase of τ. The $x_2^{(3)}$ line represents the internal stationary state as a function of τ when $\tau_C = 2\tau$, $\tau_D = \tau$. The internal stationary state's value decreases with an increase in τ. On the right, the stability of the system in the parameter space τ_C and τ_D is shown. The solid black line indicates the point of bifurcation. In the "Full Cooperation" region, only e_1 is stable. In the "Coexistence" region, only e_2 is stable, the fraction of cooperators indicated by the colour. The values considered on the left are represented by dashed ($x_2^{(1)}$), dotted ($x_2^{(2)}$) and dot-dashed ($x_2^{(3)}$) lines, respectively. The effects of only one delay present can be observed on the left and bottom edges of the plot.

$$\tilde{x}_2 = \frac{1}{c^2\tau_D}\Big(b(2-2c\tau_D) + 2c^2\tau_D + c\tau_D - c - \sqrt{b^2(4-8c\tau_D) + 4bc(2c\tau_D + \tau_D - 1) + c^2(\tau_D - 1)^2}\Big) = \lim_{\tau_C \to 0} x_2^*. \tag{49}$$

In the limit of defector delay tending to 0, the internal stationary state approaches $x_2 = (b-c)/(b-c/2)$. In the purple region of Fig. 3 two internal stationary states can be present, corresponding to e_2 and e_3 such that $\tilde{x}_2$ is given by Eq. (49) and $\tilde{x}_3$ by:

$$\tilde{x}_3 = \frac{1}{c^2\tau_D}\Big(b(2-2c\tau_D) + 2c^2\tau_D + c\tau_D - c + \sqrt{b^2(4-8c\tau_D) + 4bc(2c\tau_D + \tau_D - 1) + c^2(\tau_D - 1)^2}\Big) = \lim_{\tau_C \to 0} x_2^*. \tag{50}$$

In the limit of no delays present, only one of the internal stationary states exists in the interval $(0, 1)$, in particular, $\lim_{\tau_D \to 0} \tilde{x}_2 = (b-c)/(b-c/2)$.

If only cooperators experience delays ($\tau_D = 0$) the system (19) has one possible internal stationary state $\bar{e}_2$. The value of $\bar{x}_2$ is equal to the stationary state value x_2^* in the limit of no defector delays:

$$\bar{x}_2 = \frac{1}{4b^2\tau_C}\Big(2b\tau_C - 2b + c + \sqrt{8b^2\tau_C(2b-2c) + (2b\tau_C - 2b + c)^2}\Big) = \lim_{\tau_D \to 0} x_2^*. \tag{51}$$

With the cooperator delay approaching 0, the value of the internal stationary state approaches the no-delay value: $\lim_{\tau_C \to 0} \bar{x}_2 = x_2 = (b-c)/(b-c/2)$.

Examples. We perform numerical analysis on two payoff matrices, each corresponding to one region in Fig. 3. Matrix (52) ($b = 5$ and $c = 2$) corresponds to the grey region and the matrix (53) ($b = 5$, $c = 3.9$) lies in the purple region.

$$\begin{array}{cc} C & D \\ C \\ D \end{array} \begin{pmatrix} R = 4 & S = 3 \\ T = 5 & P = 0 \end{pmatrix} \tag{52}$$

In the case of no delays, the game characterised by the payoff matrix (52) has one stable stationary state $x = 0.75$ and two unstable stationary states of full cooperation and full defection.

In Fig. 4, the behaviour of the internal stationary state is analysed. In most of the space, the internal stationary state exists and is stable. The internal stationary state disappears above the boundary value of τ_D, and full cooperation becomes stable. To showcase the dynamics in the purple region of Fig. 3, we look at another payoff matrix:

$$\begin{array}{cc} C & D \\ C \\ D \end{array} \begin{pmatrix} R = 3.05 & S = 1.1 \\ T = 5 & P = 0 \end{pmatrix} \tag{53}$$

In Fig. 5, the behaviour of the dynamics of the Snowdrift game characterised by matrix (53) is showcased. For a small interval of values of delays, i.e. $\tau_C < 0.00715429$, we can observe the coexistence of two internal stationary states that collide in a saddle–node bifurcation by increasing the delay magnitude τ_D. In the remainder of the space, the dynamics are similar to the ones observed for matrix (52).

3.3. Prisoner's Dilemma game

Lastly, we analyse the Prisoner's Dilemma. In this game, each player can choose to incur a cost c to provide the opponent with a benefit b (C) or not (D) (Doebeli and Hauert, 2005). Additionally, here, we introduce a base endowment of c so that all of the possible payoffs of the game are non-negative. Hence, the game is represented by the following matrix:

$$\begin{array}{cc} C & D \\ C \\ D \end{array} \begin{pmatrix} R = b & S = 0 \\ T = b + c & P = c \end{pmatrix} \tag{54}$$

where $b > c > 0$. If no delays are present, the game has one stable stationary state, full defection ($x_0 = 0$), no internal stationary state exists, and full cooperation ($x_1 = 1$) is unstable. For the Prisoner's Dilemma ((54)) the system (15) becomes:

$$\begin{aligned} \frac{dx(t)}{dt} &= \frac{y_C(t)(1-x(t))}{\tau_C} - \frac{y_D(t)x(t)}{\tau_D} \\ \frac{dy_C(t)}{dt} &= y_C\left(\frac{\tau_C - 1}{\tau_C} - \frac{y_C(t)}{\tau_C} - \frac{y_D(t)}{\tau_D}\right) + bx^2(t) \\ \frac{dy_D(t)}{dt} &= y_D\left(\frac{\tau_D - 1}{\tau_D} - \frac{y_C(t)}{\tau_C} - \frac{y_D(t)}{\tau_D}\right) + (bx(t) + c)(1 - x(t)) \end{aligned} \tag{55}$$

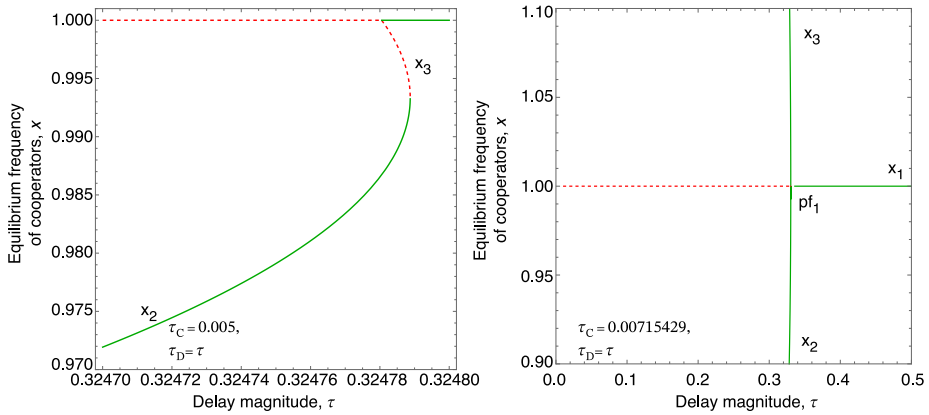

Fig. 5. The stability and the existence of internal stationary states of the Snowdrift game represented by matrix (53) depends on the time delays. The left plot represents the internal stationary states' values as a function of τ, when $\tau_C = 0.005$, $\tau_D = \tau$. Two internal stationary states may exist at the same time. The value of x_3^* decreases with τ and x_2^* increases. e_3 is always unstable and appears when full cooperation becomes stable. After the internal stationary states collide, they disappear, and full cooperation is the only stable stationary state. Full defection is always unstable. As shown on the right plot, the two internal stationary states emerge at $\tau_C = 0.00715429$, and $\tau_D \approx 0.33031257$ as the codimension-two pitchfork bifurcation unfolds into a transcritical bifurcation and the saddle–node which gives rise to e_2 and e_3. The details of these mechanisms are further investigated in Appendix B.

In the interval $[0, 1]$, three stationary states of the system (55) are possible. Full defection (equivalent to x_0) becomes:

$$e_0 = \left(0, 0, \frac{1}{2}\left(\tau_D - 1 + \sqrt{4c\tau_D + \tau_D^2 - 2\tau_D + 1}\right)\right). \tag{56}$$

In e_0, the condition (17) becomes

$$\frac{1}{2\tau_D}\left(\tau_D - 1 + \sqrt{4c\tau_D + \tau_D^2 - 2\tau_D + 1}\right) > 1. \tag{57}$$

For the condition to hold, the inequality $c \geq 1$ needs to be true. The full cooperation stationary state (equivalent to x_1) takes the following form:

$$e_1 = \left(1, \frac{1}{2}\left(\tau_C - 1 + \sqrt{4b\tau_C + \tau_C^2 - 2\tau_C + 1}\right), 0\right). \tag{58}$$

Then, in e_1 the condition (17) becomes

$$\frac{1}{2\tau_C}\left(\tau_C - 1 + \sqrt{4b\tau_C + \tau_C^2 - 2\tau_C + 1}\right) > 1, \tag{59}$$

which holds true when $b \geq 1$. Additionally, an internal stationary state appears:

$$e_2 = \left(x_2^*, \frac{\tau_C x_2^* y_D^*}{\tau_D(1 - x_2^*)}, y_D^*\right) \tag{60}$$

where

$$y_D^* = \frac{1}{2}(1 - x_2^*)\left(\tau_D - 1 + \sqrt{\tau_D(4bx_2^* + 4c - 2) + \tau_D^2 + 1}\right) \tag{61}$$

$$x_2^* = \frac{1}{2}\left(\frac{-2c\tau_C + \tau_C - \tau_D}{b\tau_C - b\tau_D} + \sqrt{\frac{-4c + \tau_C - \tau_D}{b^2(\tau_C - \tau_D)}}\right). \tag{62}$$

To ensure that the population grows exponentially, we have

$$\frac{\tau_C x_2^* y_D^*}{\tau_D \tau_C (1 - x_2^*)} + \frac{y_D^*}{\tau_D} > 1, \tag{63}$$

and $x_2^* > 1/b$. Hence, for the population to grow in each stationary state, an additional constraint on the game has to be introduced: $c \geq 1$. In the internal stationary state, the following needs to hold: $x_2^* > 1/b$.

Homogeneous stationary states. The stability analysis of the full defection stationary state e_0 shows that it always exists and is always stable. Full cooperation e_1 is unstable, unless the following is true: $\tau_D > c/(-b + b^2) \wedge \tau_C < r$ where $r = \frac{2(b-1)b\tau_D - c\left(-2b\tau_D + \tau_D + 1 + \sqrt{\tau_D(4b+4c+\tau_D-2)+1}\right)}{2(b+c-1)(b+c)}$. Full cooperation becomes stable for a big enough delay of defectors and a small enough delay of cooperators. Details of the stability analysis are presented in Appendix A.3.

Internal stationary state. The system has no internal stationary state if no delays are present. Then, for $\tau_D > c/(-b+b^2)$ and $\tau_C = r$ the internal stationary state appears at $x_2^* = 1$. A further increase in τ_D leads to a decrease in x_2^*. An increase in τ_C always leads to an increase in x_2^* until it disappears again when $\tau_C > r$. Notably, x_2^* attains positive values only if $\tau_D > \tau_C$. In the limit of defector delay approaching infinity, $\tau_D \to \infty$, x_2^* approaches a limiting value $1/b$, ensuring population growth in the internal stationary state.

One delay present. We analyse the system's behaviour when only one of the delays is present. For $\tau_C = 0$ the system (18) has one internal stationary state in the interval $(0, 1)$, which coincides with the limit of the internal stationary state x_2^*:

$$\tilde{x}_2 = \frac{1 + \sqrt{\frac{4c}{\tau_D} + 1}}{2b} = \lim_{\tau_C \to 0} x_2^*.$$

In the case of no defector delay ($\tau_D = 0$) the system (19) does not have an internal solution in the $(0, 1)$ interval. This result is explained by the fact that the existence of the internal stationary state of the general Prisoner's Dilemma depends on the presence of the defector delay. Consequently, we see that in the limit of $\tau_D \to 0$, the internal solution takes a value that is always less than 0: $\lim_{\tau_D \to 0} x_2^* = \frac{-2c+1+b\sqrt{\frac{\tau_C - 4c}{b^2 \tau_C}}}{2b} < 0$.

We show that for the Prisoner's Dilemma in the cost-benefit form (transformed for all payoffs to be non-negative), complete defection is always stable, regardless of the delays. However, it is possible for full cooperation to become stable and for the unstable internal stationary state to appear. If both extreme stationary states are stable, an increase in the strategy's delay leads to a decrease in the size of the basin of attraction of the respective stationary state.

Examples. For the numerical analysis, we use the following payoff matrix:

$$\begin{array}{cc} & \begin{array}{cc} C & D \end{array} \\ \begin{array}{c} C \\ D \end{array} & \begin{pmatrix} R = 3 & S = 0 \\ T = 5 & P = 2 \end{pmatrix} \end{array} \tag{64}$$

Fig. 6 explores the change in the system stability in the parameter space of delays. In the majority of the parameter space full defection is the only stable stationary state. As the delay of defectors increases, full cooperation becomes stable, as indicated by the colourful region in the plot, the colours representing the value of the internal stationary state.

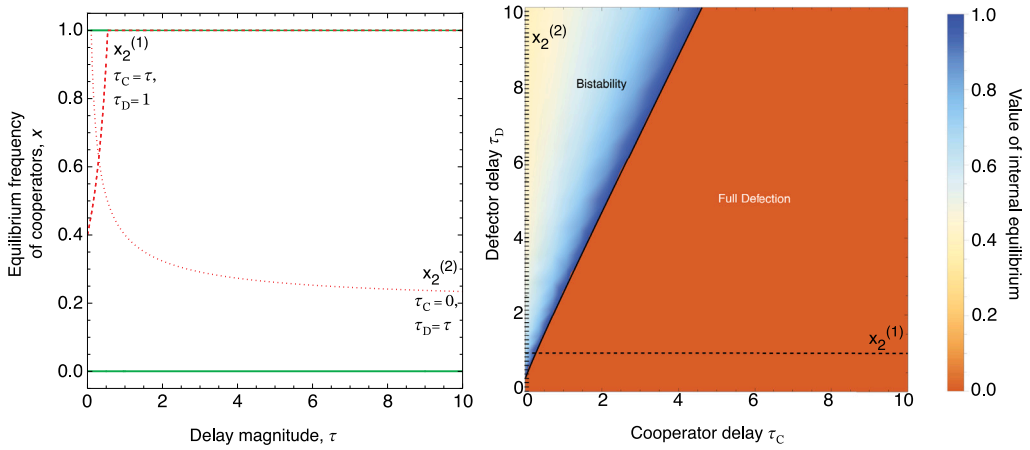

Fig. 6. Stability of the stationary states of the Prisoner's Dilemma represented by matrix (64). On the left, the stationary state values for specific values of delays are plotted. The dashed line represents the internal stationary state $x_2^{(1)}$ as a function of τ, when $\tau_C = \tau$, $\tau_D = 1$. An increase in τ leads to an increase in stationary state value. The internal stationary state ceases to exist for a high enough value of τ, and full cooperation is not stable anymore. The dotted line represents internal stationary state $x_2^{(2)}$ as a function of τ, when $\tau_C = 0, \tau_D = \tau$. Full defection is the only stable stationary state for small values of τ, and no internal stationary state exists. With the increase in τ, the internal stationary state appears, and full cooperation becomes stable. The value of the internal stationary state decreases with the increase of τ. On the right, the stability of the system in the parameter space τ_C and τ_D is shown. The solid black line indicates the point of the bifurcation. In the "Full Defection" region, only e_0 is stable. In the "Bistability" region, both e_0 and e_1 are stable, and their basins of attraction are divided by the unstable internal stationary state. The colour indicates the value of the internal stationary state. The values considered on the left are represented by dashed ($e_2^{(1)}$) and dotted ($e_2^{(1)}$) lines, respectively. The effects of only one delay present can be observed on the left and bottom edges of the plot.

4. Conclusions

Differential equations with time delays are infinite-dimensional dynamical systems, and therefore, any analytical solutions are difficult to obtain. Still, delays are ubiquitous in nature and, as such, should not be ignored in modelling. Here, we presented a different approach to model time delays in replicator dynamics of evolutionary games. In our Kindergarten model, strategy-dependent time delays correspond to rates at which offspring leave the corresponding kindergarten and are able to play games. Our qualitative results coincide with conclusions presented in Miękisz and Bodnar (2021) while providing benefits of lower complexity and more accessible analysis.

We derive explicit formulas for the stationary fraction of cooperators in the population. Namely, we show that in the Stag–Hunt game, a strategy delay leads to a decrease in the size of its basin of attraction of the corresponding absorbing state. High enough cooperator time delay destabilises full cooperation. The same cannot be said about full defection, which is stable regardless of delay values. Similar behaviour can be observed in the Prisoner's Dilemma game. With the introduction of time delays, full cooperation can become locally asymptotically stable. Again, it is not possible to destabilise full defection.

In both games, cooperation can be leveraged when we introduce stochasticity in finite populations. According to the "one-third rule" (Nowak et al., 2004), generalised in Nałęcz-Jawecki and Miękisz (2018), a strategy can be evolutionarily stable in finite populations if its basin of attraction is bigger than $1/3$ (the fixation probability of the competing strategy is smaller than the inverse of the population size). Therefore, by increasing the basin of attraction, delays can give the cooperators the needed advantage to take over the population. The Snowdrift game represents a reverse situation to the Stag–Hunt and Prisoner's Dilemma ones — full defection can never be stable. However, full cooperation can become stable. If the internal stationary state exists, it is stable, and its value depends on the delays. An increase in the delay of a given strategy decreases its fraction in the coexistence stationary state. Moreover, an additional second internal stationary state may appear.

The effects of delays are not limited to shifting internal stationary states within the game class, but additionally, they can lead to a change in the nature of the game itself. We show that introducing strategy-dependent delays alters the effective games played and subsequently leads to a change of optimal strategies. This result underlines the importance of considering the temporal structure of studied systems. Our approach can be used in games with multiple strategies and multi-player games.

CRediT authorship contribution statement

Małgorzata Fic: Writing – review & editing, Writing – original draft, Visualization, Methodology, Investigation, Formal analysis, Conceptualization. **Frank Bastian:** Writing – review & editing, Visualization, Investigation, Formal analysis. **Jacek Miękisz:** Writing – review & editing, Investigation, Conceptualization. **Chaitanya S. Gokhale:** Writing – review & editing, Writing – original draft, Supervision, Investigation.

Declaration of competing interest

The authors declare that they have no known competing financial interests or personal relationships that could have appeared to influence the work reported in this paper.

Acknowledgements

MF thanks Javad Mohamadichamgavi, Péter Bayer, and Stefano Giaimo for the fruitful discussions. Funding from the Max Planck Society, Germany is graciously acknowledged. This research is supported by the European Union's Horizon 2020 research and innovation programme under the Marie Skłodowska-Curie grant under the grant agreement number 955708.

Appendix A. Stability analysis

A.1. Stag–Hunt

We perform a stability analysis of the Stag–Hunt game's full defection stationary state e_0. Its eigenvalues are given by:

$$\lambda_{0,1} = -\frac{\sqrt{4b\tau_D + \tau_D^2 - 2\tau_D + 1}}{\tau_D} \tag{A.1}$$

$$\lambda_{0,2} = -\frac{\tau_D - 1 + \sqrt{4b\tau_D + \tau_D^2 - 2\tau_D + 1}}{2\tau_D} \tag{A.2}$$

$$\lambda_{0,3} = \frac{\tau_D + 1 - \sqrt{4b\tau_D + \tau_D^2 - 2\tau_D + 1}}{2\tau_D} - \frac{1}{\tau_C}. \tag{A.3}$$

This stationary state is always stable.

In contrast, the full cooperation stationary state e_1 can change its stability. The eigenvalues of the stationary state are given by:

$$\lambda_{1,1} = -\frac{\sqrt{(4a-2)\tau_C + \tau_C^2 + 1}}{\tau_C} \tag{A.4}$$

$$\lambda_{1,2} = \frac{1 - \sqrt{4a\tau_C + \tau_C^2 - 2\tau_C + 1}}{2\tau_C} - \frac{1 + \sqrt{4b\tau_D + \tau_D^2 - 2\tau_D + 1}}{2\tau_D} \tag{A.5}$$

$$\lambda_{1,3} = \frac{1 - \sqrt{(4a-2)\tau_C + \tau_C^2 + 1}}{2\tau_C} - \frac{1 - \sqrt{4b\tau_D + \tau_D^2 - 2\tau_D + 1}}{2\tau_D}. \tag{A.6}$$

The change in the stability of the stationary state happens via transcritical bifurcation when $\lambda_{1,3} = 0$, which takes place when $\tau_C = m$. At this point, we observe the internal stationary state reaching the full cooperation stationary state ($e_1 = e_2$) and the stability of the two stationary states exchanges. For $\tau_C \geq m$, the full cooperation stationary state e_1 is unstable, and e_2 does not exist. When e_2 exists, it is unstable, and the full cooperation stationary state is stable.

A.2. Snowdrift game

First, we present the stability analysis of the full cooperation stationary state e_1 of the Snowdrift game. The eigenvalues are given by:

$$\lambda_{1,1} = -\frac{\sqrt{4b\tau_C - 2(c+1)\tau_C + \tau_C^2 + 1}}{\tau_C} \tag{A.7}$$

$$\lambda_{1,2} = \frac{1 - \sqrt{4b\tau_C - 2(c+1)\tau_C + \tau_C^2 + 1}}{2\tau_C} - \frac{1 + \sqrt{(4b-2)\tau_D + \tau_D^2 + 1}}{2\tau_D} \tag{A.8}$$

$$\lambda_{1,3} = \frac{1 - \sqrt{4b\tau_C - 2(c+1)\tau_C + \tau_C^2 + 1}}{2\tau_C} - \frac{1 - \sqrt{(4b-2)\tau_D + \tau_D^2 + 1}}{2\tau_D}. \tag{A.9}$$

The change in stability of the stationary state happens via a transcritical bifurcation when $\lambda_{1,3} = 0$. The bifurcation takes place when $\tau_D = n$. At this point, we observe one of the internal stationary states (e_2 or e_3 depending on the parameter values) and the full cooperation stationary state exchange stability. For $\tau_D > n$, full cooperation is a stable stationary state.

We perform the stability analysis of the full defection stationary state e_0. The eigenvalues are given by:

$$\lambda_{0,1} = -\frac{|\tau_D - 1|}{\tau_D} \tag{A.10}$$

$$\lambda_{0,2} = -\frac{1 + \sqrt{\tau_C(4b-4c-2) + \tau_C^2 + 1}}{2\tau_C} + \frac{1 - |\tau_D - 1|}{2\tau_D} \tag{A.11}$$

$$\lambda_{0,3} = -\frac{1 - \sqrt{\tau_C(4b-4c-2) + \tau_C^2 + 1}}{2\tau_C} + \frac{1 - |\tau_D - 1|}{2\tau_D}. \tag{A.12}$$

The stationary state changes its stability via a transcritical bifurcation when $\lambda_{0,3} = 0$, which occurs when $\left(b < c + 1 \wedge \tau_D = p\right)$. The full defection stationary state is stable if $\left(b < c + 1 \wedge \tau_D > p\right)$ and unstable otherwise. For the model assumptions not to be violated, we assume that $b < c + 1$ and hence, the full defection stationary state e_0 is always unstable.

A.3. Prisoner's Dilemma

We perform the stability analysis of the full defection stationary state e_0. The eigenvalues of the stationary state are given by:

$$\lambda_{0,1} = -\frac{\sqrt{(4c-2)\tau_D + \tau_D^2 + 1}}{\tau_D} \tag{A.13}$$

$$\lambda_{0,2} = -\frac{\tau_D - 1 + \sqrt{(4c-2)\tau_D + \tau_D^2 + 1}}{2\tau_D} \tag{A.14}$$

$$\lambda_{0,3} = \frac{1 - \sqrt{4c\tau_D + \tau_D^2 - 2\tau_D + 1}}{2\tau_D} + \frac{\tau_C - 2}{2\tau_C}. \tag{A.15}$$

The full defection stationary state is always stable.

Now, we perform the analysis of the full cooperation stationary state e_1. The eigenvalues are given by:

$$\lambda_{1,1} = -\frac{\sqrt{(4b-2)\tau_C + \tau_C^2 + 1}}{\tau_C} \tag{A.16}$$

$$\lambda_{1,2} = -\frac{1 + \sqrt{\tau_D(4b+4c-2) + \tau_D^2 + 1}}{2\tau_D} + \frac{1 - \sqrt{(4b-2)\tau_C + \tau_C^2 + 1}}{2\tau_C} \tag{A.17}$$

$$\lambda_{1,3} = -\frac{1 - \sqrt{\tau_D(4b+4c-2) + \tau_D^2 + 1}}{2\tau_D} + \frac{1 - \sqrt{(4b-2)\tau_C + \tau_C^2 + 1}}{2\tau_C}. \tag{A.18}$$

Full cooperation can change its stability via a transcritical bifurcation when $\lambda_{1,3} = 0$, which takes place when $\{\tau_D > c/(-b+b^2) \wedge \tau_C = r\}$. At the bifurcation point, we have $e_1 = e_2$ and the internal stationary state exchanges stability with a full cooperation stationary state. For $\tau_D > c/(-b+b^2) \wedge \tau_C < r$ full cooperation is stable. In this parameter region, the internal stationary state e_2 exists in the relevant interval ($x_2^* \in (1,0)$) and is unstable. Outside this parameter space, stationary state e_2 does not exist, and full cooperation is unstable.

Appendix B. Unfolding of pitchfork bifurcations in the Kindergarten model

We recall from Fig. 5 that depending on τ_C (and the considered bifurcation parameter τ_D) either two internal equilibria (e_2 and e_3)

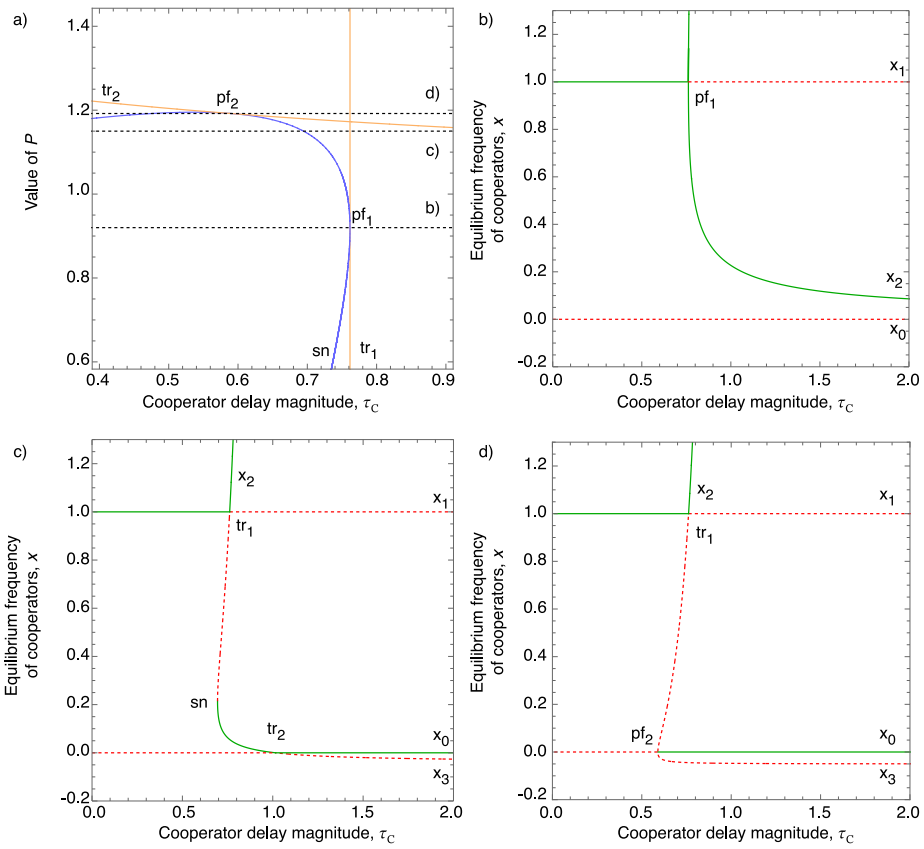

Fig. B.7. (a) The two-dimensional bifurcation diagram displays the continuation of the saddle–node bifurcation *sn* (blue) and transcritical bifurcations tr_1, tr_1 (orange) with respect to (τ_C, P). (b) At $P \approx 0.91624$, $\tau_C \approx 0.761597$, the saddle–node bifurcation *sn* collides with tr_1 in a supercritical bifurcation pitchfork pf_1. (c) Two internal equilibria e_2 and e_3 are present until either leaves the relevant interval $x^* \in [0, 1]$ via a transcritical bifurcation and the corresponding pure strategy equilibria e_0 or e_1. Particularly, e_2 bifurcates with e_1 at tr_1 and e_3 with e_0 at tr_2. (d) The saddle node bifurcation *sn* collides with the second transcritical bifurcation tr_2 in a supercritical pitchfork bifurcation at $P \approx 1.19206938$ and $\tau_C = 0.589708546$. The one-dimensional bifurcation diagrams are obtained for $P = 0.91624$ in (b), $P = 1.15$ in (c), $P = 1.19206938$ in (d) and indicated as dashed lines in (a). The remaining parameter values are $R = 3.05$, $S = 1.1$, $T = 5$, and $\tau_D = 2.0$.

or only one internal equilibrium (e_2) exists for the same Snowdrift game represented by matrix (53). Here, we would like to further illustrate the mechanism behind that observation in more detail. To do so, we consider a less restricted parameter regime in the form of a general payoff matrix (1) where its entries might serve as bifurcation parameters similar to Fig. 3.

Note that this might imply switching from one game to another. For example, in the case that the inequality $P < S$ becomes $P > S$, a Snowdrift game would change into a Prisoner's Dilemma. We use the payoff matrix (53) as a case study and consider P as an additional bifurcation parameter while keeping $R = 3.05, R = 1.1$, and $T = 5$ fixed, implying that if we vary $P > 1.1$, the Snowdrift game becomes a Prisoner's Dilemma.

Starting with $P = 0$ and $\tau_D = 2$, we consider τ_C as bifurcation parameter and continue the branch e_2 depicted in Fig. 4 for $x_2 > 1$. We observe at $\tau_C \approx 0.65833239$ a saddle–node bifurcation *sn* that gives rise to e_2 (and e_3). Throughout the following discussion, we are particularly interested in the location of this saddle–node bifurcation *sn* and track it on the (P, τ_C) parameter plane (given in Fig. B.7(a) by the blue curve).

At $P \approx 0.91624583$, and $\tau_C \approx 0.761597$ the saddle–node bifurcation *sn* collides with the transcritical bifurcation tr_1 (depicted orange Fig. B.7(a)), forming a codimension-two supercritical pitchfork bifurcation pf_1; see Fig. B.7(b). The further increase in P causes the pitchfork bifurcation pf_1 to unfold into the former saddle–node bifurcation *sn* and the transcritical bifurcation tr_1. This causes the formation of two internal stationary states e_2 and e_3 similar to Fig. 5 until e_3 bifurcates at tr_1 with e_1. Or in other words, we observe two internal equilibria e_2 and e_3 for $\tau_{sn} < \tau_C < \tau_{tr_1}$ where τ_{sn} denotes the value of τ_C of the saddle node bifurcation and accordingly τ_{tr_1} to the value of τ_C of the transcritical bifurcation tr_1.

It appears that the existence of two internal equilibria is quite robust for Snowdrift games as indicated in Fig. 3 and also noted by Miękisz and Bodnar (2021) for the original DDE model.

However, we also observed two internal states in a Prisoner's Dilemma. For example, the one-dimensional bifurcation diagram of τ_C with $P = 1.15$, given in Fig. B.7(c), we observe two internal stationary between $\tau_{sn} < \tau_C < \tau_{tr_1}$. In addition, we observe a second transcritical bifurcation tr_2, caused by e_3 colliding with e_0. Finally, further increasing of P results in a collision of *sn* with tr_2 in a subcritical pitchfork bifurcation at $P \approx 1.19206938$ and $\tau_C \approx 0.589708546$ (see Fig. B.7(d)) and the loss of two internal equilibria.

Appendix C. Extinction in a Snowdrift game due to time delay

In Appendix B, we presented the emergence of two internal equilibria that might be present in a Snowdrift game or a Prisoner's Dilemma by using a general payoff matrix (1) and considered P as an additional bifurcation parameter. Here, we want to present another bifurcation scenario that can occur in the kindergarten model and consider the following general payoff matrix

$$\begin{array}{c} \\ C \\ D \end{array} \begin{array}{c} \begin{array}{cc} C & D \end{array} \\ \begin{pmatrix} R = 2.0 & S = 0.5 \\ T = 2.95 & P = 0.01 \end{pmatrix} \end{array}, \tag{C.1}$$

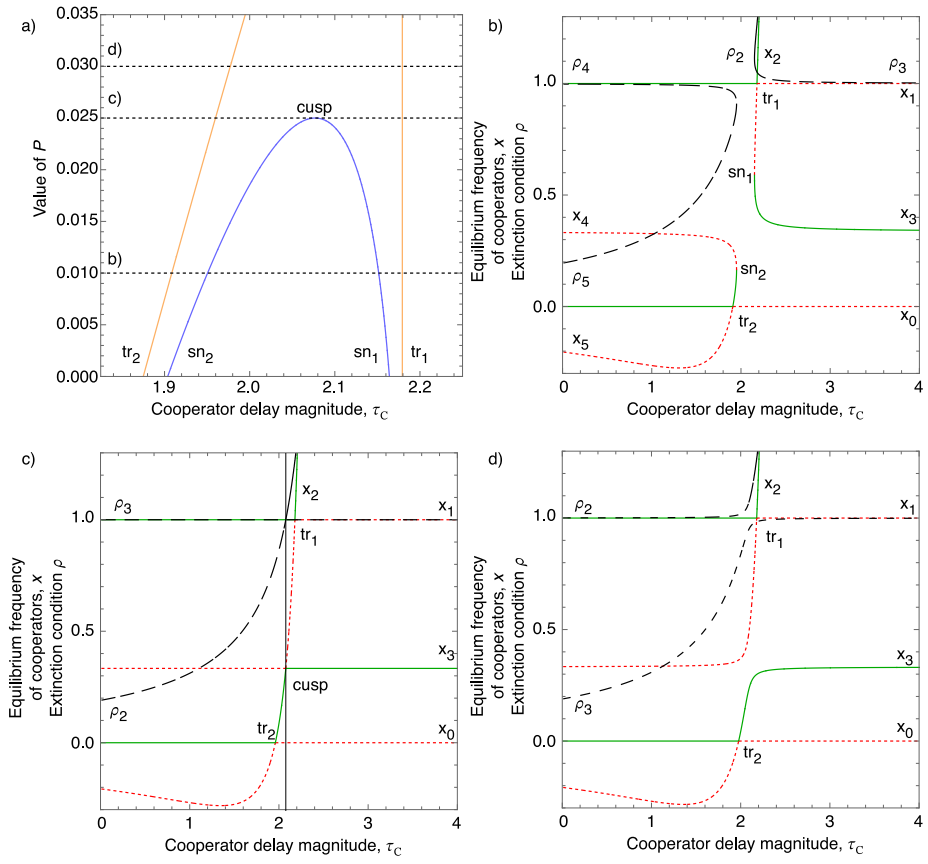

Fig. C.8. (a) The two-dimensional bifurcation diagram displays the continuation of the saddle–node bifurcations sn_1, sn_2 (blue) and transcritical bifurcations tr_1, tr_1 (orange) with respect to (τ_C, P). The saddle–node bifurcations sn_1, sn_2 collide in a cusp bifurcation for $\tau_C \approx 2.07708$, $P \approx 0.025$. (b) The two saddle node bifurcations sn_1, sn_2 give rise to two internal equilibria each. The branches e_4 and e_5 are associated with an decreasing population since $\rho_4 < 1$ and $\rho_5 < 1$ (black dashed lines) while the branches e_2 and e_3 are associated with an increasing population since $\rho_2 > 1$ and $\rho_3 > 1$ (black dashed lines). (c) At the cusp bifurcation, the population of e_3 remains constant since $\rho_3 = 1$, while the growth of population of e_2 depends on the time delay τ_C, i.e. for $\tau_C < 2.07708$ the population goes extinct and grows otherwise. (d) The detaching of e_2 and e_3 leads to an extinct population for sufficiently large enough time delay, since for $\tau_C > 2.17929238$ only e_3 remains as a single attractor in the interval $x^* \in (0, 1)$ and is associated with a decreasing population. The one-dimensional bifurcation diagrams are obtained for $P = 0.01$ in (b), $P = 0.025$ in (c), $P = 0.03$ in (d) and indicated as dashed lines in (a). The remaining parameter are $R = 2.0$, $S = 0.5$, $T = 2.95$, and $\tau_D = 5.0$.

where P serves as an additional bifurcation parameter to the delay magnitude τ_C while keeping $\tau_D = 5.0$ fixed.

We start by varying τ_C while keeping $P = 0.01$ fixed. The corresponding bifurcation diagram is depicted in Fig. C.8(b). Similar to Fig. 5 and Appendix B, we observe two internal equilibria e_2 and e_3 for $\tau_{sn_1} < \tau_C < \tau_{tr_1}$, where τ_{sn_1} denotes the value of τ_C of the saddle node bifurcation sn_1 and accordingly τ_{tr_1} the value of τ_C of the transcritical bifurcation tr_1. In addition and akin to the region $\tau_{sn_1} < \tau_C < \tau_{tr_1}$, we observe two internal equilibria e_5 and e_6 for $\tau_{tr_2} < \tau_C < \tau_{sn_2}$ but with inverted stabilities compared to e_2 and e_3. Moreover, due to e_4 being repelling, we observe a bistable region for $0 < \tau_C < \tau_{tr_2}$ in a Snowdrift Game. To investigate whether the population is at risk of extinction, we recall the extinction condition from Eq. (17)

$$\rho(e^*, \tau_C, \tau_D) = \frac{y_C^*(t)}{\tau_C} + \frac{y_D^*(t)}{\tau_D} > 1, \tag{C.2}$$

and write ρ_* to denote the extinction condition Eq. (17) associated with e^*. We observe that both equilibria e_2 and e_3 correspond to a growing population indicated by $\rho_2 > 1$ and $\rho_3 > 1$ (both depicted as black dashed lines in Fig. C.8(b)). In contrast, e_4 and e_5 correspond to a population with a risk of extinction since $\rho_4 < 1$ and $\rho_5 < 1$. In other words, the bistability observed in the Snowdrift Game is due to a repelling (extinct) population of e_4. To summarise, we observe for the Snowdrift Game given in Equation and increasing delay magnitude τ_C, a change from bistability to two (extinction) equilibria e_4 and e_5, to full cooperation, to two (alive) equilibria e_2 and e_3, to a single stable mixed equilibrium e_3.

Next, and similar to Appendix B, we increase the payoff P in the general payoff matrix , whereas the corresponding bifurcation diagram of the (P, τ_C) parameter plane is given in Fig. C.8(a). We observe that the scenario of Fig. C.8(b) persists until sn_1 and sn_2 collide at a cusp bifurcation for $\tau_C \approx 2.07708$, $P \approx 0.025$. At the cusp point, sn_1 and sn_2 are connected via a transcritical bifurcation for varying τ_C (see Fig. C.8(c)). Note that in this degenerated case, the population of the connecting branch x_3 remains constant since $\rho_3 = 1$. Moreover, note that e_2 is stable for $\tau_{tr_2} < \tau_C < \tau_{cusp}$ but its population is decreasing since $\rho_2 < 1$ in this interval of τ_C. On the other hand, e_2 is repelling for $\tau_{cusp} < \tau_C < \tau_{tr_1}$ but its population is growing since $\rho_2 > 1$ in this interval of τ_C.

A further increase of P results in a detaching of e_2 and e_3, as depicted in Fig. C.8(d) with $P = 0.03$. The branch e_2 is repelling separating cooperating and defection for $\tau_C < \tau_{tr_1}$, where τ_{tr_1} denotes the value of the transcritical bifurcation tr_1 and e_2 leaving the relevant interval of $x_3^* \in (0, 1)$. As indicated by $\rho_2 > 1$, the population of e_2 is growing. In contrast, $\rho_3 < 1$ and the population associated with e_3 is at risk of extinction. Note that e_3, is attractive for $\tau_C > \tau_{tr_2}$, where tau_{tr_2} denotes the value of τ_C for the transcritical bifurcation tr_2 and e_2 entering the relevant interval of $x_2^* \in (0, 1)$. Or to sum things up, for $\tau_C > \tau_{tr_2}$, e_2 remains as single attractor and its population is decreasing.

Code availability

Appropriate computer code describing the model and used to produce the figures is available on GitHub at https://github.com/tecoevo/compartmentalised_timedelays.

References

Alboszta, J., Miękisz, J., 2004. Stability of evolutionarily stable strategies in discrete replicator dynamics with time delay. J. Theoret. Biol. 231 (2), 175–179.

Bateson, P., 1994. The dynamics of parent–offspring relationships in mammals. Trends Ecol. Evolut. 9 (10), 399–403.

Ben-Khalifa, N., El-Azouzi, R., Hayel, Y., 2018. Discrete and continuous distributed delays in replicator dynamics. Dyn. Games Appl. 8 (4), 713–732.

Binswanger, J., Carman, K.G., 2012. How real people make long-term decisions: The case of retirement preparation. J. Econ. Behav. Organ. 81 (1), 39–60.

Bodnar, M., Miękisz, J., Vardanyan, R., 2020. Three-player games with strategy-dependent time delays. Dyn. Games Appl. 10 (3), 664–675.

Bourne, Jr., L.E., 1957. Effects of delay of information feedback and task complexity on the identification of concepts. J. Exp. Psychol. 54 (3), 201–207.

Doebeli, M., Hauert, C., 2005. Models of cooperation based on the Prisoner's Dilemma and the snowdrift game. Ecol. Lett. 8, 748–766.

Glendinning, P., 1994. Stability, Instability and Chaos: An Introduction to the Theory of Nonlinear Differential Equations. Cambridge University Press.

Iijima, R., 2011. Heterogeneous information lags and evolutionary stability. Math. Social Sci. 61 (2), 83–85.

Iijima, R., 2012. On delayed discrete evolutionary dynamics. J. Theoret. Biol. 300, 1–6.

Kaiser, T.S., von Haeseler, A., Tessmar-Raible, K., Heckel, D.G., 2021. Timing strains of the marine insect clunio marinus diverged and persist with gene flow. Mol. Ecol. 30 (5), 1264–1280.

Khalifa, N.B., El-Azouzi, R., Hayel, Y., Mabrouki, I., 2016. Evolutionary games in interacting communities. Dyn. Games Appl. 7 (2), 131–156.

Lauenroth, D., Gokhale, C.S., 2023. Theoretical assessment of persistence and adaptation in weeds with complex life cycles. Nat. Plants.

Maynard Smith, J., Price, G.R., 1973. The logic of animal conflict. Nature 246, 15–18.

Miękisz, J., Bodnar, M., 2021. Evolution of populations with strategy-dependent time delays. Phys. Rev. E 103 (1), 012414.

Miękisz, J., Matuszak, M., Poleszczuk, J., 2014. Stochastic stability in three-player games with time delays. Dyn. Games Appl. 4 (4), 489–498.

Miękisz, J., Mohamadichamgavi, J., Vardanyan, R., 2023. Small time delay approximation in replicator dynamics. arXiv:2303.08200.

Miękisz, J., Poleszczuk, J., Bodnar, M., Urszula, F., 2011. Stochastic models of gene expression with delayed degradation. Bull. Math. Biol. 73 (9), 2231–2247.

Miękisz, J., Wesolowski, S., 2011. Stochasticity and time delays in evolutionary games. Dyn. Games Appl. 1 (3), 440–448.

Moreira, J.A., Pinheiro, F.L., Nunes, A., Pacheco, J.M., 2012. Evolutionary dynamics of collective action when individual fitness derives from group decisions taken in the past. J. Theoret. Biol. 298.

Nałęcz-Jawecki, P., Miękisz, J., 2018. Mean-potential law in evolutionary games. Phys. Rev. Lett. 120, 028101.

Nowak, M.A., Sasaki, A., Taylor, C., Fudenberg, D., 2004. Emergence of cooperation and evolutionary stability in finite populations. Nature 428 (6983), 646–650.

Oaku, H., 2002. Evolution with delay. Jpn. Econ. Rev. 53 (1), 114–133.

Osborne, M.J., et al., 2004. An Introduction to Game Theory, vol. 3. Oxford University Press, New York.

Serra, C.R., Earl, A.M., Barbosa, T.M., Kolter, R., Henriques, A.O., 2014. Sporulation during growth in a gut isolate of bacillus subtilis. J. Bacteriol. 196 (23), 4184–4196.

Skyrms, B., 2004. The Stag Hunt and the Evolution of Social Structure. Cambridge University Press.

Veltz, R., 2020. BifurcationKit.jl. URL https://hal.archives-ouvertes.fr/hal-02902346.

Wesson, E., Rand, R., 2016. Hopf bifurcations in delayed rock–paper–scissors replicator dynamics. Dyn. Games Appl. 6 (1), 139–156.

Wesson, E., Rand, R., Rand, D., 2016. Hopf bifurcations in two-strategy delayed replicator dynamics. Int. J. Bifurc. Chaos 26 (01), 1650006.

Wettergren, T.A., 2023. Replicator dynamics of evolutionary games with different delays on costs and benefits. Appl. Math. Comput. 458, 128228, URL https://www.sciencedirect.com/science/article/pii/S0096300323003971.

Yi, T., Zuwang, W., 1997. Effect of time delay and evolutionarily stable strategy. J. Theoret. Biol. 187 (1), 111–116.